Measurement 236 (2024) 114980

Contents lists available at ScienceDirect

Measurement

journal homepage: www.elsevier.com/locate/measurement

# New IEC standards for the measurement of sheet resistance on large-area graphene using the van der Pauw and the in-line four-point probe methods

Alessandro Cultrera [a,c,*], Danilo Serazio [a], Norbert Fabricius [b,c], Luca Callegaro [a]

[a] Quantum Metrology and Nanotechnologies, Istituto Nazionale di Ricerca Metrologica (INRIM), Strada delle Cacce, 91, Torino, 10135, Italy
[b] ISC –International Standards Consulting GmbH & Co., Verdistrasse, 15A, Gehrden, D-30989, Germany
[c] IEC – International Electrotechnical Commission, Technical Committee 113 "Nanotechnology for Electrotechnical Products and Systems", Switzerland

ARTICLE INFO

*Keywords:*
Graphene
Repeatability
Electrical properties
Standardization

ABSTRACT

Graphene has evolved from a scientific research subject to an industrial product, in need of a normative basis for its key control characteristics. Recently two new IEC technical specifications that establish standardized procedures for assessing the sheet resistance $R_S$ of monolayer graphene have been published. These new standards, part of the IEC TS 62607-6-xx series, outline protocols for employing two contact methods: i) van der Pauw, and ii) in-line four-point probe. In the following we present and discuss illustrative examples of the scientific experiments designed and performed to inform the standardization process behind the presented standards. In particular we report about the investigation of mechanical contacting of chemical-vapor-deposited monolayer graphene and the measurement of the $R_S$ in $cm^2$ area graphene samples with non uniform resistivity distributions. This paper includes an overview of the broader IEC context, detailing the key steps in the development of the standards themselves.

## 1. Introduction

Once graphene was unambiguously isolated in laboratory in 2004 [1], immediately academic research focused on its basic properties and industry begun to develop and place on the market several types of graphene and related products. The field progressed on even more encouraging results since the first evidence on academic journals of large-scale graphene synthesis [2] by chemical vapor deposition (CVD) in 2009. Still today, graphene used in academic research is hardly comparable to the raw materials offered by the industrial providers. Even within the same laboratory or industrial firm, repeatability and definition of materials' representative parameters (key control characteristics) is an issue that still holds. In fact, many available synthesis processes — such as mechanical exfoliation, chemical vapor deposition and reduction of graphene oxide dispersion, yield "graphene" with very different properties: graphene synthesized in labs rather than the one produced in industry has flakes of different size, possibly containing several types of defects and chemical contamination; research on scalable graphene is indeed facing a reproducibility gap [3].

For a successful uptake of products involving graphene and related materials, the availability of international standards is essential to define the key material properties and the appropriate measurement protocols. Within this framework, at the International Electrotechnical Commission, the Technical Committee 113 "Nanotechnology for electrotechnical products and systems" (IEC/TC 113) added the standardization of graphene and related materials into its work programme as early as 2012. The task was allocated to the Working Group 8 "Graphene related materials/Carbon nanotube materials". Currently, 36 graphene related standards either published or under development are within the IEC/TC 113. Focusing on the electrical properties of graphene, IEC/TC 113 established a liaison with the GRACE[1] research consortium [4], and since 2017 several standards about the electrical characterization of graphene were initiated within this interaction, see the BOX 1.

* Corresponding author at: Quantum Metrology and Nanotechnologies, Istituto Nazionale di Ricerca Metrologica (INRIM), Strada delle Cacce, 91, Torino, 10135, Italy.
*E-mail addresses:* a.cultrera@inrim.it (A. Cultrera), d.serazio@inrim.it (D. Serazio), norbert.fabricius@isc-team.eu (N. Fabricius), l.callegaro@inrim.it (L. Callegaro).

[1] EMPIR 16NRM01 GRACE "Developing electrical characterization methods for future graphene electronics". EMPIR is the European Metrology Programme for Innovation and Research, funded by EURAMET, the European Association of National Metrology Institutes.

https://doi.org/10.1016/j.measurement.2024.114980
Received 29 February 2024; Received in revised form 29 April 2024; Accepted 21 May 2024
Available online 23 May 2024

*BOX 1 - Published IEC Standards on four-probe contact methods for the measurement of $R_S$.*

**IEC TS 62607-6-7:2023** Nanomanufacturing - Key control characteristics - Part 6–7: Graphene - Sheet resistance: van der Pauw method.

**IEC TS 62607-6-8:2023** Nanomanufacturing - Key control characteristics - Part 6–8: Graphene - Sheet resistance: in-line four-point probe.

The collaboration between IEC/TC 113 and the GRACE consortium has significantly contributed to the comprehensive framework for the electrical characterization of graphene, beyond the foundational measurements of sheet resistance. This synergy has led to the development of standards that address a variety of Key Control Characteristics (KCCs), enhancing the scope and utility of graphene in technological applications. Particularly noteworthy are efforts to supplement established sheet resistance measurement techniques. Alongside the more consolidated methods as the van der Pauw (vdP), the in-line four-point (4PP) and the time-domain terahertz spectroscopy (TDS), innovative approaches are being explored to provide a comprehensive set of standardized graphene electrical properties. For instance, the Gated Transfer Length Method (GTL) offers insights into charge carrier mobility and contact resistance, critical parameters for the development of high-performance electronic devices. Moreover, the introduction of methodologies like the Conductive Probe Atomic Force Microscopy (CP-AFM) for resistance measurement at the nano scale showcases the committee's dedication to advancing precision in graphene characterization. This technique, underpinned by the development of standards such as PNW TS 113–784, allows for the standardized investigation of graphene's electrical properties at the micro and nano levels, paving the way for innovations in nano electronics.

These advancements reflect the IEC/TC 113's integrated approach to graphene standardization, addressing not only sheet resistance but also other vital KCCs like contact resistance, carrier mobility, and material heterogeneity. Such efforts ensure that the international standards keep pace with the evolving landscape of graphene research and its applications across industries.

The paper is organized as follows. In Section 2 some relevant aspects about KCC in graphene (Section 2.1) and the IEC standardization process will be described (Section 2.2). In Section 3 the scientific background and technical input to the IEC TC 113 will be exemplified and thoroughly discussed for two recently published standards. In particular, in Section 3.1 the problem of purely mechanical contacting of monolayer graphene is considered for the application of IEC TS 62607-6-7:2023 (van der Pauw method) [5] and the IEC TS 62607-6-8:2023 (in-line four point probe method) [6]; in Section 3.2 the case of the measurement of real samples with a non uniform resistivity distribution is considered for the vdP method and results are discussed.

The full list of IEC/TC 113 standards related to the measurement of sheet resistance $R_S$ is reported in Appendix.

## 2. Standardization

### 2.1. Graphene key control characteristics

A Key Control Characteristic (KCC) is a property inherent to a material or an intermediate product that could impact safety, regulatory compliance, performance, quality, reliability, or subsequent processing of the final product. Various KCCs associated with graphene concern mechanical attributes (such as elastic modulus), electrical properties (including carrier density, carrier mobility, and sheet resistance), chemical composition (notably metallic impurity content), and even biological considerations (such as skin sensitization). Some KCCs may already have corresponding standards for their measurement, while others might not. Certain KCCs are mandated by the International Electrotechnical Commission (IEC) for all types of graphene and related materials. For instance, disclosing the availability of safety documentation (Material Safety Data Sheet, MSDS) or detailing the manufacturing method. Conversely, different forms of graphene may necessitate distinct subsets of KCCs for delineation. In the case of chemically exfoliated graphene oxide dispersion, the Carbon–Oxygen ratio (C/O) serves as a pertinent KCC (to be characterized in accordance with standard IEC TS 62607-06-21:2022 [7] when necessary). The same KCC does not apply to chemically vapor-deposited monolayer graphene, where the sheet resistance ($R_S$) emerges as a relevant KCC. Characterization of CVD graphene includes available standards within the IEC 62607-06-xx series, such as IEC TS 62607-06-23 (utilizing the Hall bar method) or the recently issued IEC TS 62607-06-7 (employing the van der Pauw method) and IEC TS 62607-06-8 (in-line four-point probe), see BOX 1 and for more details.

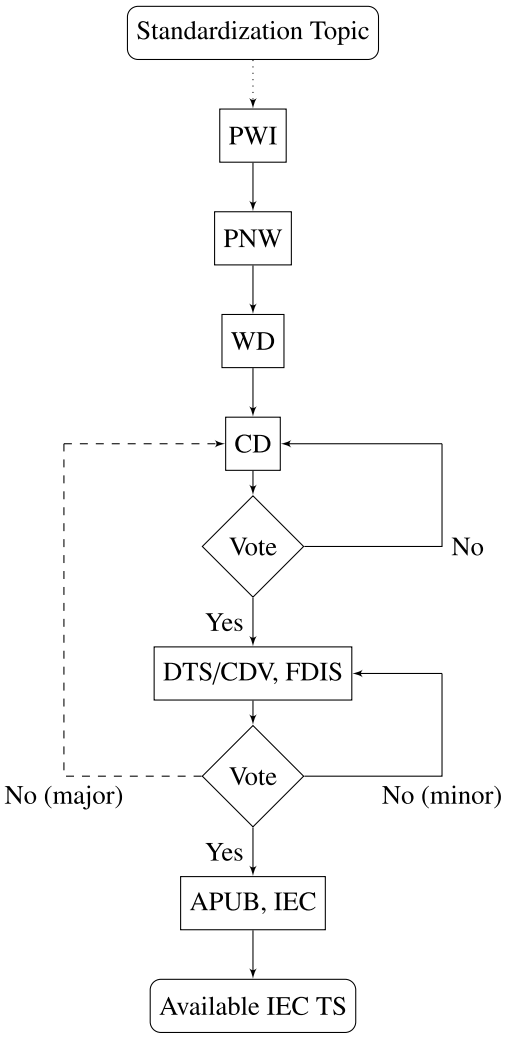


**Fig. 1.** Scheme of the development stages of IEC standards. Abbreviations are defined in BOX 2. The dotted arrow indicates that the potential standardization topic may be approved and reach the PWI stage. The loops pointing to CD and DTS represent stages where iterative discussion and revisions typically occur. The dashed loop indicates that in case of major revisions are requested, the document is returned to the CD stage.

### 2.2. IEC standards development process

The development of the standards IEC TS 62607-6-7 and IEC TS 62607-6-8 followed the IEC workflow (see Sec. 2.1.3.1. in [8]). The

main development stages are summarized in Fig. 1, the document types abbreviations are reported in the BOX 2. The process starts at the *preliminary* stage, with a standardization topic of potential interest, presented by either a TC member or an invited external expert. The topic eventually becomes a Preliminary Work Item (PWI) and is discussed at TC level within the *proposal* stage. If approved itself, the PWI becomes a New Work Item Proposal (PNW) which is then assigned a project leader (usually the author of the proposal); a project team (PT) is also formed on the basis of voluntary participation of other TC members. The PT works on a first working draft (WD) of the technical specification. When the WD prepared at PT level is considered mature enough, the technical discussion proceeds, at TC level, during the *committee stage* by iterative editing of the committee draft (CD) versions of the standard. During the technical discussion, the PT meet periodically, resolving the TC comments to the CD, eventually adding experimental and theoretical elements to bolster the document; the *committee* stage may take several iterations before the document is considered ready for the *approval* stage, where Draft Technical Specification (DTS) is considered in terms of technical contents (a DTS may also be returned to the CD stage for solving technical flaws). Once the technical discussion is concluded, two cases may occur. For Technical Specifications (lower level of consensus required) the DTS is approved for *publication* (APUB); at a higher level of consensus (required for International Standards) the DTS is approved as Committee Draft for Vote (CDV) and later, if the vote is positive, as Final Draft International Standard (FDIS) which enters the *publication* stage. Editorial and copyright revision is made on APUB documents, prior the publication as IEC documents. Each IEC standard is assigned a *stability date*, within which the document can be confirmed, revised, or withdrawn.

*BOX 2 - Abbreviations.*

**TS** Technical Specification;

**IS** International Standard;

**PWI** Preliminary Work Item;

**PNW** New Work Item Proposal;

**WD** Working Draft;

**CD** Committee Draft;

**DTS** Draft Technical Specification (TS);

**CDV** Committee Draft for Vote (IS);

**FDIS** Final Draft International Standard (IS);

**APUB, IEC** Approved For Publication;

**IEC TS** Published Technical Specification.

### 2.3. New IEC standards for graphene sheet resistance: four-point methods

CVD graphene is of particular interest in the advancement of emerging technologies, including graphene-based electronics, electrotechnical products, integration into established fabrication processes, and sensor applications. Concerning this type of graphene, the new standards IEC TS 62607-6-7 [5] and IEC TS 62607-6-8 [6], provide standardized measurement protocols for the assessment the KCC sheet resistance $R_S$ by means of contact methods: the van der Pauw (vdP, [9]) and in-line four point probe (4PP, [10]) methods.[2] The sheet resistance $R_S$, is a quantity that serves as a comprehensive indicator of the local conductivity in a sample with finite geometrical dimensions. In order for users and manufacturers to check the repeatability and consistency (with given specifications) of the electrical properties of their graphene, $R_S$ is considered a KCC for monolayer CVD graphene. IEC standards TS 62607-6-7 and TS 62607-6-8 explain how to implement standardized methods on large area from $mm^2$ to $cm^2$ CVD graphene on rigid insulating support and how to perform a reliable estimation of the sample $R_S$ and the measurement uncertainty, also considering the non-ideal nature of large-area commercial graphene; particular care has been devoted to give an estimation of $R_S$ and its uncertainty that keep into account the possible spatial variability of the electrical conductivity on a real, non-ideal sample. The two standards TS 62607-6-7 and TS 62607-6-8, cover the following aspects: (i) proper storage and preparation of samples, (ii) the required instrumentation's specifications (iii) ambient conditions during measurements, (iv) standardized procedures for performing measurements, and (v) interpretation and reporting of results. It can be noted now that the present editions of the TS 62607-6-7 and TS 62607-6-8 standardize the more established versions of the two discussed methods (4PP, vdP). Since in the field of research the implementation of these methods is continuously evolving, future editions of the presented IEC TS may consider more recent implementations (e.g. vdP implementation with simultaneous dual resistance measurement [12] which could speed up the measurements, or five-contacts implementation in which the need of contacts on the border is relaxed [13,14]).

## 3. Scientific input provided to the IEC/TC 113 for the presented standards

The GRACE research consortium designed and performed a series of experiments in order to provide quantitative scientific input to the IEC/TC 113/WG 8, backing the development of several documentary standards. In the following, two examples are reported which are related to the development of IEC TS 62607-6-7 (vdP) and IEC TS 62607-6-8 (4PP): (i) investigation on mechanical contacting of CVD graphene sheets and (ii) measurement of $R_S$ of large-area CVD graphene samples.

### 3.1. Mechanical contacting of CVD graphene

A first example of scientific evidence provided IEC/TC 113 for the discussed IEC TS is given in the following. Here is described one of the experiments performed during the TS development process, this one aimed to check the effects of purely mechanical electrical contacting on CVD graphene to perform four-point electrical measurements. Avoiding any fabrication step (lithography, etching, ...) was not only desirable, but fundamental to exclude processes that would certainly alter the pristine material conditions.

For this purpose, a custom probe equipped with four equally spaced spring-loaded tips, each featuring a round head profile, was utilized to perform four-terminal resistance measurements. The contact spot area could be estimated by SEM micrographs (see Fig. 4) to be about 30 µm, while the spacing between contacts is 3 mm. The setup also included a digital balance (Sartorius LP8200S) a lever indicator (Mitutoyo 513–404), a 3-axis moving tool and position indicator (Anilam SENC 125 linear transducers, Anilam Wizzard 411 visualizer). An HP 34401 was used in 4-wire (4W) configuration to perform resistance measurements $R_{4W}$ (from which $R_S$ can be calculated). 4W resistance is measured by applying current through the outermost tips of the test probe and

[2] New IEC standards TS 62607-6-7 and TS 62607-6-8 represent complementary standards to others of the same series describing non-contact methods (e.g. TS 62607-6-10 [11]).

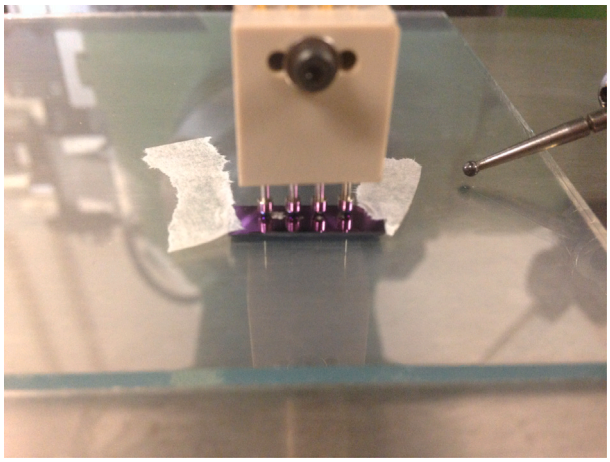

**Fig. 2.** A graphene sample is positioned atop an insulating glass slab, which rests on the balance plate. The test probe makes contact with the sample, while the lever indicator is placed in contact with the glass slab to measure the vertical displacement of the balance plate.

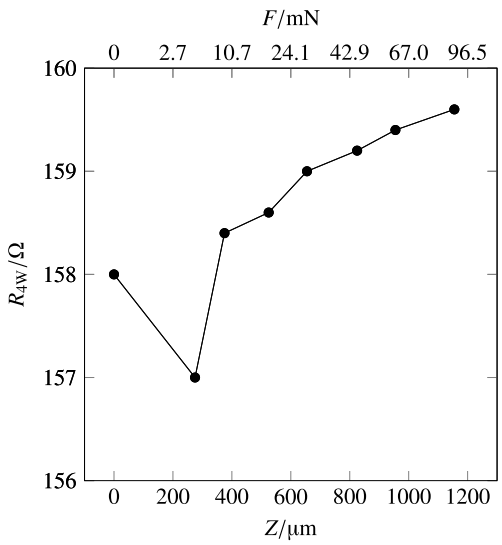


**Fig. 3.** Four-terminal resistance measurements $R_{4W}$ conducted on a graphene sample. Error bars illustrating the type B uncertainty are omitted, resulting of negligible length compared to the range of the vertical axis. The force of an individual spring is given on the top axis.

measuring the voltage drop between the two innermost tips. The probe standing on the graphene sample, the lever indicator and the balance plate are shown in Fig. 2. The sample was cut from a 4 inches wafer of commercial CVD graphene on Silicon (Pi-Kem Ltd., UK). The wafer was Boron-doped Silicon with thermal oxide coating, with graphene placed on the polished side of the wafer. The tests were conducted to assess the stability and repeatability of the electrical contact. This involved measuring both the displacement $Z$ of the probes springs and the resulting incident weight, alongside the measurement of the electrical resistance; from the measured weight and net spring displacement, the single spring force acting on the contact spot was calculated. The net displacement $Z$ of the tip springs was determined by subtracting the displacement of the balance plate from the total probe displacement measured using the moving tool. The total applied weight to the sample, which is proportional to the spring force, was measured using the weighing scale positioned under the glass slab supporting the sample. Given the rigid support and the evenly spaced probes, sample deformation was not expected to occur on substantial scale. The 4W resistance $R_{4W}$ was measured at 8 different spring $Z$, in the range 0–1155 μm (where the position 0 μm corresponds to the probe making electrical contact with the graphene) to check whether the applied force influenced the contact quality, and to assess the damage induced by the probe on the graphene layer. The 4W resistance measured[3] placing the probe at the center of the sample was $R_{4W} = 158.65\,\Omega \pm 0.85\,\Omega$. The type B uncertainty calculated from the measuring instrument's specifications was of the order of $0.05\,\Omega$.

The small measurement standard deviation suggests that the impact of spring displacement was not significant. The results of these measurements are presented in Fig. 3, which reports $R_{4W}$ as a function of the springs displacement $Z$ (and the applied force on each contact tip $F$). The plot reports a more significant change in $R_{4W}$ at smaller $Z$ values, up to approximately 300 μm, which is reasonable as the contact may be initially weaker. Subsequently, the measurements only slight increase as $Z$ values become larger; overall the total variation is of about 1%. After the electric measurements, SEM micrographs of the contacted sample were acquired to assess the damage produced by landing the test probes on the sample. The footprints of the tips, after reaching about $Z = 1.2$ mm is shown in Fig. 4. The scratched area is about 20 μm × 20 μm, which is reasonably of the order of the round tip footprint itself. Furthermore, there are at least two distinct types of damage observed: (i) regions where graphene has been peeled away, typically at the center of the landing spot (indicated by the brighter appearance of insulating thermal silicon oxide in SEM micrographs), and (ii) occasional linear shear scratches located at the base of the spot, likely resulting from lateral movement of the probe tip. The increase in the $R_{4W}$ increment shown in Fig. 3 could be attributed to the escalating damage caused by the unavoidable lateral displacement of the probe. These and comparable tests, such as verifying the repeatability of contacts by repeatedly raising and landing the probe on identical spots, indicated that mechanically making contact with monolayer graphene sheets on rigid supports was a feasible approach for standardized protocols. This feasibility is further underpinned by the fact that commercial test probes readily available on the market could be directly utilized for this purpose by most laboratories.

### *3.2. Measurement of $R_S$ of commercial, cm$^2$ size CVD graphene samples using the van der Pauw method*

A second consistent example of the work behind the development of the presented standards is represented by the investigation of the application of the vdP method to samples for which the basic assumptions of the method may be not satisfied (i.e. resistivity uniformity). Here we report the case commercial CVD graphene samples (which are expected to be uniform in principle) using purely mechanical contacting as discussed in Section 3.1.

#### *3.2.1. Basic assumptions and formulas of the vdP method*

The van der Pauw method can be applied to samples of arbitrary shape and the contacts shall be placed at the boundary of the sample. The vdP method has been demonstrated on the basis on some assumptions: (i) the sample has an isotropic and uniform resistivity, (ii) the diameter of the contacts is small compared to the sample size (point contacts) and (iii) the sample thickness is much smaller than the probe spacing (thus equivalent to a quasi-2D scenario) [9]. Understanding and considering these assumptions is crucial for obtaining accurate and reliable $R_S$ measurements using the vdP method. If any of these assumptions are violated, corrections at some extent can be applied

[3] Note that, for the sole purpose of assessing the effects of pure mechanical contacting of graphene, the measurement of $R_{4W}$ was not used to further estimate the sheet resistance $R_S$, which would include systematic errors due to the sample size compared to the probe size.

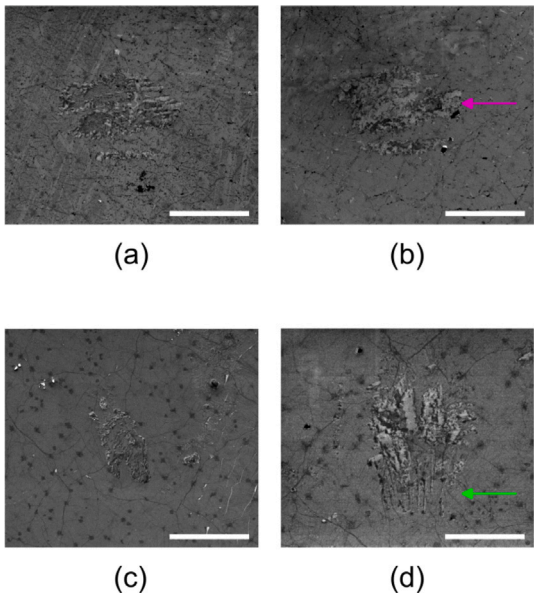


**Fig. 4.** SEM micrographs of the landing spots of the test probe tips on a monolayer CVD graphene sample on $SiO_2$. Graphene grain boundaries and multi-layer seeds are visible as darker profiles and spots. In the center of the images, the footprint of the probe tip is visible, e.g. highlighted by the magenta arrow in (b). In (a) and (d) signs of shear displacement of the tip is visible, e.g. highlighted by the green arrow in (d). Lighter gray represents areas where graphene was scratched away for the support and Silicon thermal oxide appears. Markers on the SEM images represent 25 μm.

(see [15–17] and references within) which is not always practical from the point of view of the users. In the IEC TS 62607-6-7 these aspects were considered and a reasonable practical solution is provided to the users, on the basis of typical vdP fixtures implementation. Considering the problem in more detail in the present case, the diameter of the contact spot, $\delta$, is estimated by SEM micrographs to be of about 30 μm. The ratio between the contact diameter and the sample lateral size $D$ is $\delta/D = 0.003$. This would introduce an error in the estimation of the vdP sheet resistance $R_S$ much less than 0.2% [15]. On the other hand, the contacts distance from the boundary, $d$, is 500 μm (within 10%, fixture construction accuracy). The ratio between the contact distance from the edge and the sample lateral size $D$ is $d/D = 0.05$. In the case of square samples with edge contacts, this would introduce an additional error in the estimation of $R_S$ of the order of 0.01% [18], being these estimations conservative.

The vdP measurement of $R_S$ requires the measurement of two four-terminal resistances

$$R_\alpha = \frac{V_{d,c}}{I_{a,b}}, \tag{1}$$

$$R_\beta = \frac{V_{b,c}}{I_{a,d}}, \tag{2}$$

where (a,b,c,d) are four contacts on the sample boundary. The sheet resistance $R_S$ is the calculated as

$$R_S = \frac{\pi}{\ln 2}\frac{R_\alpha + R_\beta}{2} f, \tag{3}$$

where $f$ is a numerical factor which is function of the ratio $R_\alpha/R_\beta$ [19].

### 3.2.2. Measurement of $R_S$ of samples with non-uniform resistivity distribution

In practice, implementation of point contacts and suitable experimental fixtures is often straightforward. The main limitation comes from the sample: in cm-scale CVD graphene samples, the main deviations from the basic assumption may depend indeed on the sample itself [20,21], which may have non-uniform resistivity. Additionally, the sensitivity of the vdP method is strongly position-dependent [22], which means that not only the sample discontinuity/defects is relevant, but also the position of these features influences the global vdP measurement.

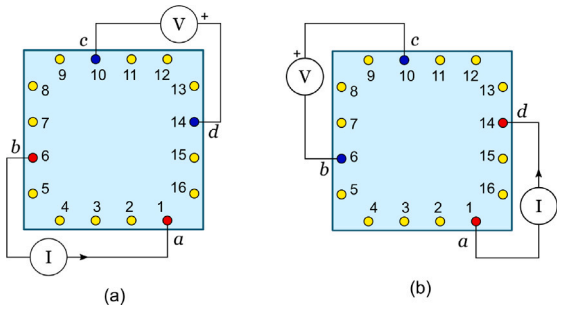


**Fig. 5.** vdP measurement using a multi terminal fixture. Connections to the current source I and the voltmeter V are shown. The light blue square represents the sample area (lateral size 1 cm); circles represent spring loaded contacts (not in scale). The contacts corresponding to the vdP measurement at (1, 6, 10, 14) involved in the measurements $R_\alpha$ (a) and $R_\beta$ (b) are shown: blue circles correspond to voltage sensing contacts, red circles correspond to current carrying contacts. Yellow circles represents other available contacts (open circuit).

In this study, vdP measurements were performed on two commercial 1 $cm^2$ CVD graphene samples (made available by the GRACE consortium) labeled S28 and S40 in the following.[4] Several four-contact vdP configurations were achieved using a multi-terminal fixture described in [23], using for each vdP configuration 4 out of the available 16 contacts.

In particular, here are considered $p = 1...P$ with $P = 256$ possible vdP configurations, including (i) consecutive contacts (1, 2; 3, 4) corresponding to $R_\alpha = R_{4,3;1,2}$ and $R_\beta = R_{2,3;1,4}$ and (ii) contacts on the edges (1, 6; 10, 14) corresponding to $R_\alpha = R_{14,10;1,6}$ and $R_\beta = R_{6,10;1,14}$; the latter configuration is represented in Fig. 5.

To distinguish among different results of $R_S$ obtained in different vdP contacts configurations, we define

$$R_S^{(p)} = \frac{\pi}{\ln 2}\frac{R_\alpha^{(p)} + R_\beta^{(p)}}{2} f, \tag{4}$$

where $p$ is the vdP measurement configuration, and define a *configurational average* of $R_S$ as

$$\overline{R_S} = \frac{1}{P}\sum_p R_S^{(p)}, \tag{5}$$

where the angled parentheses represent averaging over the $p$ measurement configurations.

Each measurement $R_S^{(p)}$ calculated from (4) in a given contact configuration $p$ has its own corresponding combined uncertainty $u(R_S^{(p)})$ which is calculated from the type A (variance) and type B (instruments specifications) uncertainty components of the measurement. Applying to (5) the law of propagation of uncertainty we can determine the uncertainty of $\overline{R_S}$ as

$$u(\overline{R_S}) = \sqrt{s^2(R_S^{(p)}) + \sum_p u^2(R_S^{(p)})}, \tag{6}$$

where $s(R_S^{(p)})$ is the standard deviation of the set $R_S^{(p)}$.

It must be noted that for the case of rigid rotation (or electronic multiplexing) with fixed position contacts, only $P/2$ configuration yield be linearly independent measurements, the others $P/2$ being reciprocal measurements (i.e the source and the sense contacts are only swapped) which would give no additional information let alone more statistics. In

[4] For consistency with previous literature [23].

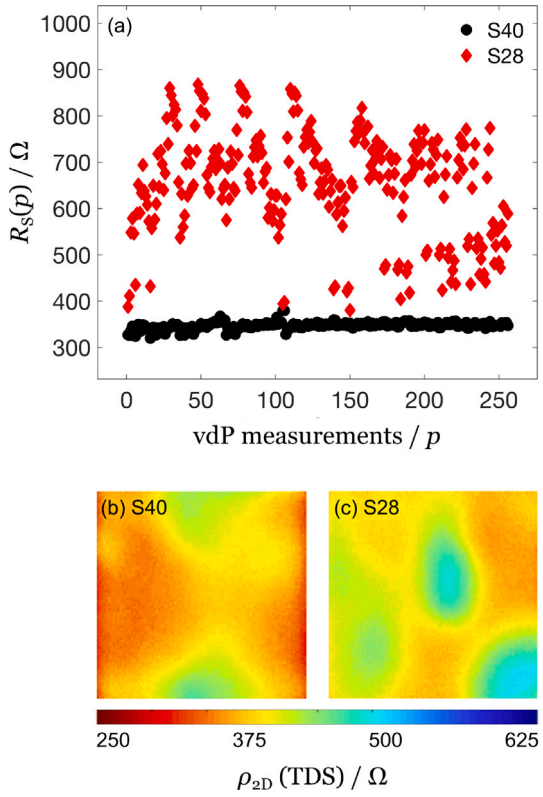


**Fig. 6.** (a) van der Pauw measurements in $P$ contact configurations for two CVD graphene samples. (b), (c) local 2D resistivity maps of the samples measured with TDS.
*Source:* Adapted with permission from [23].

a general case though (as per Fig. 5) any $p$ configuration can be chosen independent on the others.

To perform the measurements, a current source I (Keithley K2602B) and a voltmeter V (Keysight 34461) were wired to the fixture through a multiplexer Keysight 34980 equipped with a reed relay matrix board (Keysight 34933, not shown in Fig. 5), in order to switch among the $P$ vdP measurement configurations. Samples were energized with current $I = 100\,\mu A$. Each measurement was performed in forward and reverse polarization (reversing $I$) to minimize possible thermo-electric voltages. The present measurements were performed at $T = (23 \pm 0.5)°$ and $RH = (50 \pm 4\%)$ relative humidity.[5]

Fig. 6-a reports the results of the $P$ vdP measurements of $R_S^{(p)}$ for both samples S28 and S40. The two samples present rather different dispersion of the results, in particular for sample S40, $\overline{R_S} = 347.6\,\Omega$ with $s(R_S^{(p)}) = 7.3\,\Omega$ while to S28 correspond $\overline{R_S} = 652.7\,\Omega$ with $s(R_S^{(p)}) = 114.5\,\Omega$, which is a much more dispersed outcome.

The combined uncertainty $u(R_S^{(p)})$ of a single $R_S^{(p)}$ measurements on S40, considering the type A uncertainty over 10 measurements repetitions, and instruments specifications is of the order of $0.07\,\Omega$. This is, even for the sample with less dispersed results, almost two orders of magnitude smaller compared to $s(R_S^{(p)})$of S40 (hence $u(R_S^{(p)})$ is a minor contribution to $u(\overline{R_S})$). This substantial dependence of $R_S^{(p)}$ on the measurement configuration suggest that the uniformity assumptions of the vdP method are not satisfied.

[5] In particular, the range $RH = (50 \pm 4\%)$ was proposed and adopted, reaching consensus at normative level, in the presented IEC TS for vdP and 4PP. Experimental results show that the resistivity of CVD graphene $SiO_2$ is substantially affected by adsorbed water in the range 30% to 70% $RH$, with increasing conductivity with adsorbed water concentration on graphene. The mechanism underpinning graphene's sensitivity to humidity is reported to be the result of the electrostatic interaction between the water and the graphene-support system [24–26].

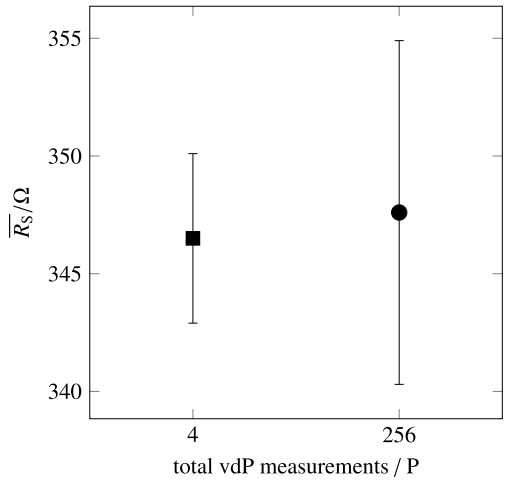


**Fig. 7.** Sheet resistance of sample S40 obtained with vdP measurements performed over 4 contacts ($P = 4$, square marker) and 16 contacts ($P = 256$, round marker). Error bars represent $u(\overline{R_S})$.

**Table 1**
$R_S^{(p)}$ measurements across 4 contacts on sample S40 and the corresponding combined uncertainty $u(R_S^{(p)})$.

| $p$ | $R_S^{(p)}/\Omega$ | $u(R_S^{(p)})/\Omega$ |
|---|---|---|
| 1 | 344.679 | 0.041 |
| 2 | 344.075 | 0.060 |
| 3 | 351.828 | 0.043 |
| 4 | 345.431 | 0.044 |

These results can be compared with resistivity maps of the same samples reported in Fig. 6-b and -c. These maps were obtained with terahertz time-domain spectroscopy (TDS) which is itself a standardized technique [11]. The TDS maps show clearly that the sample S40 is rather uniform compared to sample S28. In particular 2D resistivity of map S40 take values in the range $\rho_{2D} = 285 - 400\,\Omega$, while pixels of the TDS map of sample S28 take values in the range $\rho_{2D} = 380 - 690\,\Omega$. This difference is consistent with the vdP measurements, which for a rather uniform sample like S40 still give reasonable results ($R_S^{(p)}$ dependents weakly on $p$), while give unreliable results for a non-uniform sample like S28 ($R_S^{(p)}$ strongly depends on $p$). Note that in practice, users even at research institutions level, perform vdP measurements with fixtures with four-contacts in fixed position (see for example [27]), allowing at best four different contact configurations only (square samples). In this case, it is likely to obtain very different results on non-uniform samples. Note that TDS maps were carried out prior to any mechanical contacting of the samples with the multi-terminal contact array; the fact that both TDS and vdP measurements on samples are in agreement (S40 more uniform, S28 less uniform) suggest that any substantial effect of contact tip damage (see Section 3.1) can be excluded.

All this considered, vdP could be considered not suitable for samples which are not guaranteed to be uniform. Yet the aim of the new IEC TS 62607-6-7 was to mitigate the limitation of the vdP method. In fact vdP is more established, straightforward and cost-accessible for industry-users (the typical stakeholders of documentary standards) than other techniques with spatial resolution. It is shown in the following that the definition given in (5) can be useful to get meaningful results also in practical cases when a typical four-contact fixture is used.

Fig. 7 reports $\overline{R_S}$ of S40 measured across 4 contacts and 16 contacts (from data of Fig. 6-a). In the four-contact scenario we measured S40 using only the contacts (1,6,10,14) of the fixture schematized in Fig. 5.

**Table A.2**
IEC/TC 113 standards related to graphene's sheet resistance, $R_S$.

| Publication date | Edition | IEC reference | Title |
|---|---|---|---|
| Under development | 1 | IEC TS 62607-6-23 | Nanomanufacturing - Key control characteristics - Part 6-23: Graphene film - Sheet resistance, Carrier density, Carrier mobility: Hall bar. |
| Under development | 1 | IEC TS 62607-6-32 | Nanomanufacturing – Key control characteristics – Part 6-32: Two-dimensional materials – Charge carrier mobility, contact resistance, sheet resistance, doping, and hysteresis: Gated transfer length method. |
| Under development | 1 | PWI 113–154 | Nanomanufacturing – Key control characteristics – Part 6-37: Graphene materials – Hall resistance – Charge carrier mobility and majority. |
| Under development | 1 | PNW TS 113–784 | Nanomanufacturing - Key control characteristics - Part 10-2: Nanoelectronic devices - Resistance: conductive probe atomic force microscopy. |
| 2016 | 1 | IEC TS 62607-6-4:2016 | Nanomanufacturing - Key control characteristics - Part 6-4: Graphene - Surface conductance measurement using resonant cavity. |
| 2020 | 1 | IEC TS 62607-6-1:2020 | Nanomanufacturing - Key control characteristics - Part 6-1: Graphene-based material - Volume resistivity: four probe method. |
| 2021 | 1 | IEC TS 62607-6-10:2021 | Nanomanufacturing - Key control characteristics - Part 6-10: Graphene-based material - Sheet resistance: Terahertz time-domain spectroscopy. |
| 2022 | 1 | IEC TS 62607-6-5:2022 | Nanomanufacturing - Key control characteristics - Part 6-5: Graphene-based materials - Contact and sheet resistance: transmission line measurement. |
| 2022 | 1 | IEC TS 62607-6-9:2022 | Nanomanufacturing - Key control characteristics - Part 6-9: Graphene-based material - Sheet resistance: Eddy current method. |
| 2023 | 1 | IEC TS 62607-6-7:2023 | Nanomanufacturing - Key control characteristics - Part 6-7: Graphene - Sheet resistance: van der Pauw method. |
| 2023 | 1 | IEC TS 62607-6-8:2023 | Nanomanufacturing - Key control characteristics - Part 6-8: Graphene - Sheet resistance: In-line four-point probe. |

This returned four measurements of $R_S^{(p)}$ with $P = 4$; results are reported in Table 1 along their combined uncertainty $u(R_S^{(p)})$. The average over the $P$ configurations is $\overline{R_S} = 346.5\,\Omega$ with uncertainty $u(\overline{R_S}) = 3.7\,\Omega$. Note that also in this case the uncertainty on the configurational average is much larger than the uncertainty on the single measurement configuration, $u(\overline{R_S}) \gg u(R_S^{(p)})$. On the opposite, note that in case of a uniform sample where $s(R_S^{(p)})$ is negligible, the uncertainty of the configurational average $\overline{R_S}$ would be compatible with the uncertainty of the electrical measurement $u(R_S^{(p)})$, that is $u(\overline{R_S}) \simeq u(R_S^{(p)})$.

In general, the appropriate number of contacts (and thus of the $P$ vdP combinations) to achieve a correct estimate of $R_S$ is dependent on the sample geometry and non-homogeneity. The compatibility of different $R_S$ values given by considering different subsets of the $P$ contacts can provide confidence in measurements performed with the smaller number of contacts (for example, when considering large batches of similar samples). In summary, it has been shown that the measurement of $R_S$ obtained with 4 contacts (typical implementation) using the proposed estimation of uncertainty is compatible with the measurement performed with the 16 contacts fixture of this study, and yet takes into account by a large amount the effect of spatial variability.

The definitions discussed this section were proposed to the technical committee TC/113 and are implemented in the present version of the IEC TS 62607-6-7; at stability date (see Section 2.2) better solutions could be considered, discussed an possibly implemented once agreed by the TC experts.

## 4. Conclusion

Exploring new concepts in the laboratory based on original ideas is crucial for scientific progress. However, standardization is essential to translate these scientific advancements into production. In this work we highlighted some of the scientific background behind the development of IEC TS 62607-6-7 (van der Pauw) and IEC TS 62607-6-8 (in-line four-point probe). The presented new standards for the electrical characterization of the KCC $R_S$ of CVD graphene can contribute to the establishment of shared good practices and standardized measurement protocols in research labs and industry.

## CRediT authorship contribution statement

**Alessandro Cultrera:** Writing – review & editing, Writing – original draft, Visualization, Validation, Supervision, Software, Methodology, Investigation, Conceptualization. **Danilo Serazio:** Writing – review & editing, Investigation, Conceptualization. **Norbert Fabricius:** Writing – review & editing, Writing – original draft, Methodology, Conceptualization. **Luca Callegaro:** Writing – review & editing, Writing – original draft, Supervision, Resources, Methodology, Investigation, Conceptualization.

## Declaration of competing interest

The authors declare the following financial interests/personal relationships which may be considered as potential competing interests: Luca Callegaro reports financial support was provided by EURAMET European Metrology Programme for Innovation and Research. Norbert Fabricius reports a relationship with International Standards Consulting GmbH & Co. KG that includes: employment. If there are other authors, they declare that they have no known competing financial interests or personal relationships that could have appeared to influence the work reported in this paper.

## Data availability

Data will be made available on request.

## Acknowledgments

The work has been done within the Joint Resarch Projects i) 16NRM01 GRACE – Developing electrical characterisation methods for future graphene electronics; ii) 20FUN03 COMET – Two dimensional lattices of covalent- and metal-organic frameworks for the Quantum Hall resistance standard. These projects received funding from the EMPIR programme co-financed by the Participating States and from the European Union's Horizon 2020 research and innovation programme.

## Appendix. Full list of IEC standards related to $R_S$

The list in Table A.2 reports the IEC/TC 113 standards related to the measurement of sheet resistance $R_S$. These include contact and non-contact methods and may overlap with other KCCs like e.g. carrier mobility or contact resistance. Some are more recent projects still under development (PWI, PNW), others have been already published as TS. All these document are relatively recent and at their first edition, which may progress as stability date revisions may occur (see Section 2.2).

## References


[1] K.S. Novoselov, et al., Electric field effect in atomically thin carbon films, Science 306 (5696) (2004) 666–669.

[2] X. Li, et al., Large-area synthesis of high-quality and uniform graphene films on copper foils, Science 324 (5932) (2009) 1312–1314.

[3] P. Bøggild, Research on scalable graphene faces a reproducibility gap, Nature Commun. 14 (1) (2023) 1126.

[4] L. Callegaro, C. Cassiago, A. Cultrera, V. D'Elia, D. Serazio, M. Ortolano, M. Marzano, O. Kazakova, C. Melios, F. Raso, et al., GRACE: Developing electrical characterisation methods for future graphene electronics, in: 2018 Conference on Precision Electromagnetic Measurements (CPEM 2018), IEEE, 2018, pp. 1–2.

[5] IEC TS 62607-6-7:2023, Nanomanufacturing - Key Control Characteristics - Part 6-7: Graphene - Sheet Resistance: van der Pauw Method, IEC, Geneve, Switzerland.

[6] IEC TS 62607-6-8:2023, Nanomanufacturing - Key Control Characteristics - Part 6-8: Graphene - Sheet Resistance: In-Line Four-Point Probe, IEC, Geneve, Switzerland.

[7] IEC TS 62607-6-21:2020, Nanomanufacturing - Key Control Characteristics - Part 6-21: Graphene - Elemental Composition, C/O Ratio: X-Ray Photoelectron Spectroscopy, IEC, Geneve, Switzerland.

[8] ISO/IEC Directives Part 1, Procedures for Technical Work, IEC, Geneve, Switzerland, 2022.

[9] L.J. van der Pauw, A method of measuring the resistivity and hall coefficient on lamellae of arbitrary shape, Philips Tech. Rev. 20 (1958) 220–224.

[10] F. Smits, Measurement of sheet resistivities with the four-point probe, Bell Syst. Tech. J. 37 (3) (1958) 711–718.

[11] IEC TS 62607-6-10:2021, Nanomanufacturing - Key Control Characteristics - Part 6-10: Graphene - Sheet Resistance: Terahertz Time-Domain Spectroscopy, IEC, Geneve, Switzerland.

[12] L. Pantleon, et al., Simultaneous dual-configuration van der Pauw measurements of gated graphene devices, Measurement 225 (2024) 113954.

[13] K.R. Szymański, P.A. Zaleski, Determination of the sheet resistance of an infinite thin plate with five point contacts located at arbitrary positions, Measurement 169 (2021) 108360.

[14] K.R. Szymański, P.A. Zaleski, M. Kondratiuk, Five-probe method for finite samples-an enhancement of the van der Pauw method, Measurement 217 (2023) 113039.

[15] R. Chwang, B.J. Smith, C.R. Crowell, Contact size effects on the van der pauw method for resistivity and hall coefficient measurement, Solid State Electron. 17 (1974) 1217–1227.

[16] D.S. Perloff, Four-point sheet resistance correction factors for thin rectangular samples, Solid State Electron. 20 (1977) 681–687.

[17] I. Miccoli, F. Edler, H. Pfnür, C. Tegenkamp, The 100th anniversary of the four-point probe technique: the role of probe geometries in isotropic and anisotropic systems, J. Phys.: Condens. Matter. 27 (22) (2015) 223201.

[18] D.W. Koon, A.A. Bahl, E.O. Duncan, Measurement of contact placement errors in the van der Pauw technique, Rev. Sci. Instrum. 60 (2) (1989) 275–276.

[19] A.A. Ramadan, R.D. Gould, A. Ashour, On the van der Pauw method of resistivity measurements, Thin Solid Films 239 (1994) 272–275.

[20] P. Bøggild, et al., Mapping the electrical properties of large-area graphene, 2D Mater. 4 (4) (2017) 042003.

[21] Christos Melios, Nathaniel Huang, Luca Callegaro, Alba Centeno, Alessandro Cultrera, Alvaro Cordon, Vishal Panchal, Israel Arnedo, Albert Redo-Sanchez, David Etayo, et al., Towards standardisation of contact and contactless electrical measurements of CVD graphene at the macro-, micro-and nano-scale, Sci. Rep. 10 (1) (2020) 3223.

[22] D.W. Koon, C.J. Knickerbocker, What do you measure when you measure resistivity? Rev. Sci. Instrum. 63 (1) (1992) 207–210.

[23] Alessandro Cultrera, Danilo Serazio, Amaia Zurutuza, Alba Centeno, Oihana Txoperena, David Etayo, Alvaro Cordon, Albert Redo-Sanchez, Israel Arnedo, Massimo Ortolano, et al., Mapping the conductivity of graphene with Electrical Resistance Tomography, Sci. Rep. 9 (1) (2019) 10655.

[24] A.D. Smith, et al., Resistive graphene humidity sensors with rapid and direct electrical readout, Nanoscale 7 (45) (2015) 19099–19109.

[25] Y. Yang, R. Murali, Binding mechanisms of molecular oxygen and moisture to graphene, Appl. Phys. Lett. 98 (9) (2011) 093116.

[26] T.O. Wehling, A.I. Lichtenstein, M.I. Katsnelson, First-principles studies of water adsorption on graphene: The role of the substrate, Appl. Phys. Lett. 93 (20) (2008) 202110.

[27] G. Rietveld, et al., Dc conductivity measurements in the van der Pauw geometry, IEEE Trans. Instrum. Meas. 52 (2003) 449–453.